

STUDY OF RADIATION INDUCED DEEP-LEVEL DEFECTS IN PROTON IRRADIATED AlGaAs-GaAs SOLAR CELLS*

Sheng S. Li
University of Florida
Gainesville, Florida

EXTENDED ABSTRACT

The purpose of this paper is to report our findings on the study of the radiation induced deep-level defects (both electron and hole traps) in the proton irradiated AlGaAs-GaAs p-n junction solar cells and to show the correlation between the measured defect parameters and the solar cell performance parameters. This work was carried out in collaboration with Dr. Loo of Hughes Research Labs in conjunction with their high efficiency GaAs solar cell program for space applications. The range of proton energies was from 50 KeV to 10 MeV and the proton fluence was varied from 10^{10} to 10^{13} P/cm². Experimental tools employed include deep-level transient spectroscopy (DLTS), capacitance-voltage (C-V), current voltage (I-V), and SEM-EBIC methods. Defect and recombination parameters such as defect density and energy level, capture cross section, carrier lifetimes and effective hole diffusion lengths in n-GaAs LPE layers have been determined from these measurements. Detailed discussions of the measurement techniques and experimental results on the proton induced defects in GaAs solar cells can be obtained from our recent NASA technical reports and publications listed in ref. 1 through ref. 6. Highlights of our technical findings are summarized as follows:

(1) From the DLTS and C-V measurements, it is found that (a) the defect density (both electron and hole traps) increases with increasing proton fluence, (b) 50 KeV protons only produced damages in the p-AlGaAs window layer and the p-GaAs LPE layer and showed the least degradation to the solar cell performance, (c) the most severe damages were created by protons with energies between 200 and 300 KeV in which defect densities were high and defect spectrum was complicated; on the other hand, the defect density in the 0.8 and 10 MeV proton irradiated samples was lower and the defect spectrum was simpler than those samples with lower proton energies, (d) the dominant electron trap levels observed are the $E_c-0.52$ eV and $E_c-0.71$ eV, which are the main recombination centers in these proton-irradiated samples; increasing the proton fluence will result in the increase in the amplitude of $E_c-0.52$ eV level and the reduction of $E_c-0.71$ eV level. Fig. 1 and Fig. 2 show the DLTS spectra as a function of proton energy for the electron and hole traps, respectively, for proton fluences of 10^{12} P/cm². It is clearly illustrated in both figures that defect spectra in the 200 KeV and 290 KeV proton irradiated samples are more complex than those in the 100 KeV and 10 MeV samples. Fig. 3 and Fig. 4 show the DLTS spectra for the electron and hole traps, respectively as a function of proton energy, for proton fluence of 10^{13} P/cm². The dominant electron trap in this case is due to the $E_c-0.52$ eV level while the main hole trap is due to the $E_v + 0.52$ eV level. The effect of thermal annealing on the deep-level defects in

the 200 KeV proton irradiated samples has also been studied by using a 300°C thermal annealing in vacuum for one hour. The results show that defects produced by the 200 KeV protons can be effectively reduced or annealed out for proton fluences less than 10^{12} P/cm²; this is illustrated in Fig. 5. From the dark forward I-V measurements, it is found that the recombination current in the junction space charge region of the cell dominates the dark current and its magnitude increases with increasing proton fluence. The increase in the dark current with proton fluence has been attributed to the increase in the density of recombination centers in the depletion region of the cell with increasing proton fluence, as was confirmed by the DLTS data shown above. 300°C thermal annealing process reduces the dark current significantly, as is shown in Fig. 6. Fig. 7 shows the effective carrier lifetimes in the junction space charge region vs. proton fluence for two proton energies (i.e. 100 and 200 KeV), as calculated from the dark forward I-V data shown in Fig. 6. The results show that carrier lifetimes vary from around 4 ns for the unirradiated cell to less than 0.1 ns as proton fluence increases to 10^{13} P/cm². A 300°C thermal annealing recovers the effective lifetime from 0.2 ns to about 1 ns. From the results of the SEM-EBIC measurements, it was found that the effective hole diffusion lengths in the n-GaAs LPE layers were reduced from around 3 μ m for the unirradiated cell to less than 0.5 μ m for the 10^{13} P/cm² and 290 KeV proton irradiated cell. A quantitative comparison between the measured defect parameters and the solar cell performance parameters shows good correlation existed between these two sets of parameters.

In short, the research finding from this work would indeed provide a useful information to guide the design of a radiation hardened GaAs solar cell for space applications, and gain a better understanding of the deep-level traps and the role of these deep-level defects on the proton irradiated solar cell performance.

*Research supported by NASA grant NSG-1425.

REFERENCES

1. S. S. Li: "Studies of Electronic Properties in proton Irradiated AlGaAs-GaAs Solar Cells." NASA Semi-Annual Technical Report, Sept. 1, (1978), (1979), and (1980).
2. S. S. Li, W. L. Wang, P. W. Lai, T. R. Owen, R. Y. Loo and S. Kamath: J. Elec. Matr. 9, 335 (1980).
3. S. S. Li, W. L. Wang, P. W. Lai, R. Y. Loo, G. S. Kamath, and R. C. Knechtli: Proc. IEEE Photovoltaic Specialist, Conf. Pp. 1080-84 (1980).
4. S. S. Li, W. L. Wang, P. W. Lai, R. Y. Loo, G. S. Kamath: IEEE Trans. Elec. Devices. ED-27, 857 (1980).
5. S. S. Li, D. W. Schoenfeld, T. T. Chiu and R. Y. Loo: Proc. of the 15th Intersociety Energy Conversion Engineering Conf.. Vol. 1, pp 354-357 (1980).
6. S. S. Li, T. T. Chiu, D. W. Schoenfeld, and R. Y. Loo: Proc. of the 11th International Conf. on Defects and Radiation Effects in Semiconductors. Sept. 8-11 (1980).

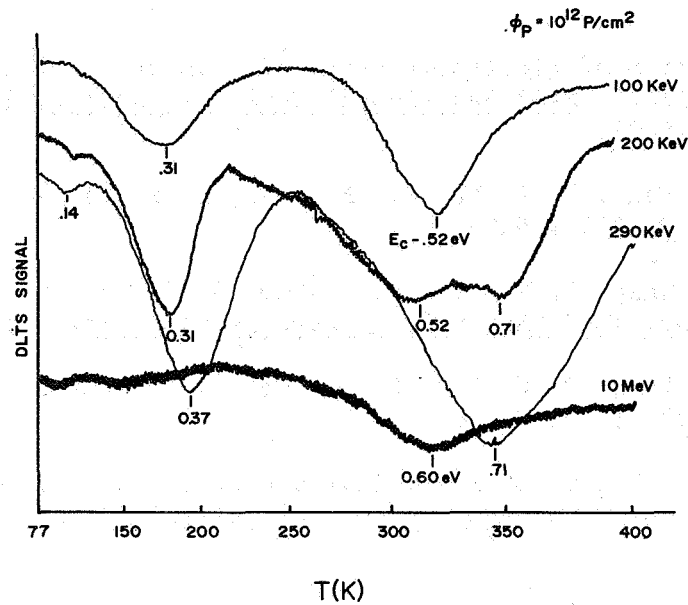


Fig. 1 DLTS scans of electron traps in proton irradiated AlGaAs-GaAs solar cells as a function of proton energy, for proton fluence of 10^{12} P/cm^2 .

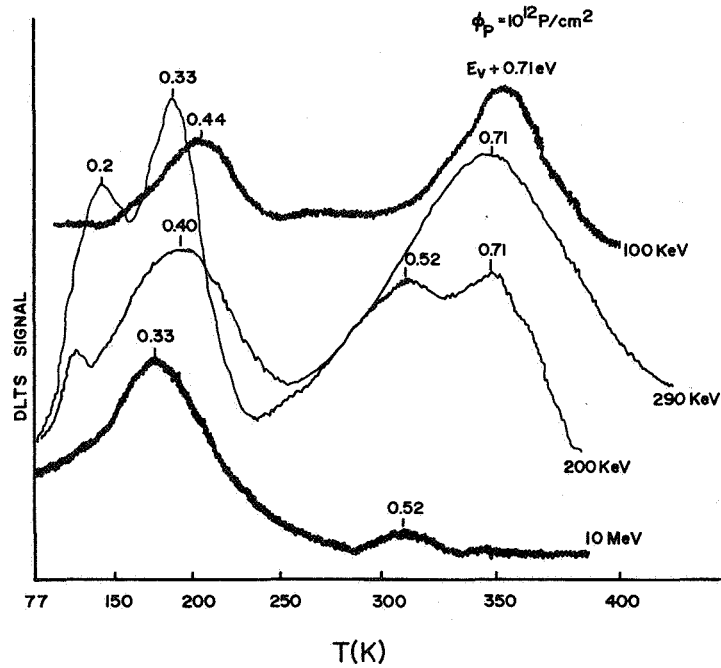


Fig. 2 DLTS scans of hole traps in proton irradiated AlGaAs-GaAs solar cells as a function of proton energy, for proton fluence of 10^{12} P/cm^2 .

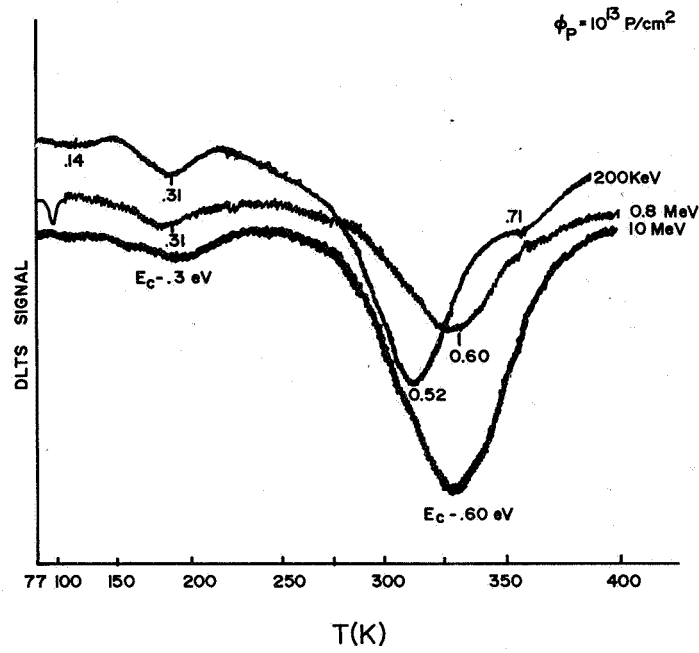


Fig. 3 DLTS scans of electron traps in proton irradiated AlGaAs-GaAs solar cells as a function of proton energy, for proton fluence of 10^{13} P/cm^2 .

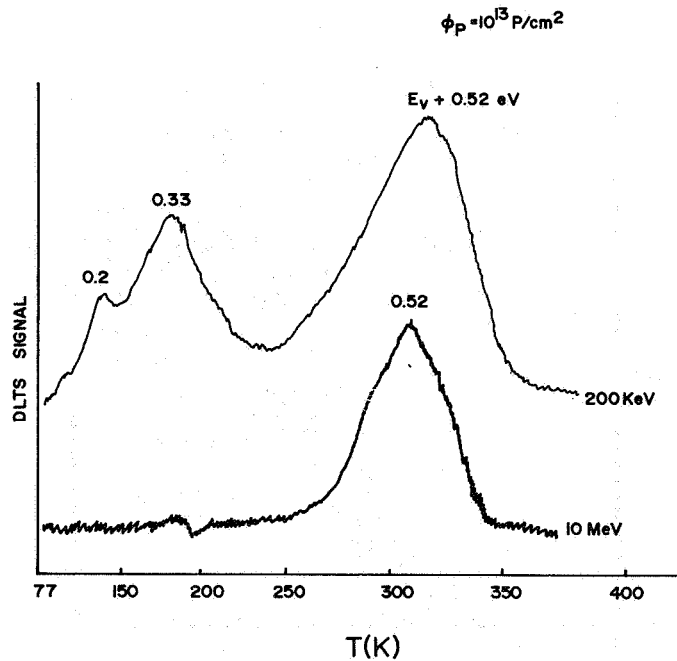


Fig. 4 DLTS scans of hole traps in proton irradiated AlGaAs-GaAs solar cells as a function of proton energy, for proton fluence of 10^{13} P/cm^2 .

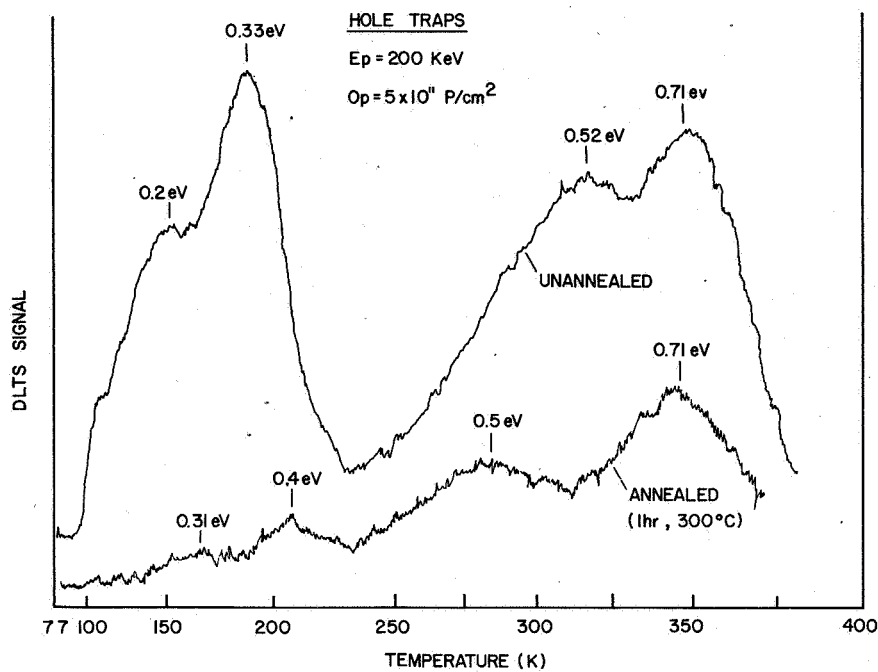


Fig. 5 DLTS scans of hole traps in 200 KeV proton irradiated AlGaAs-GaAs solar cells before and after 300°C thermal annealing, for proton fluence of 5×10^{11} P/cm².

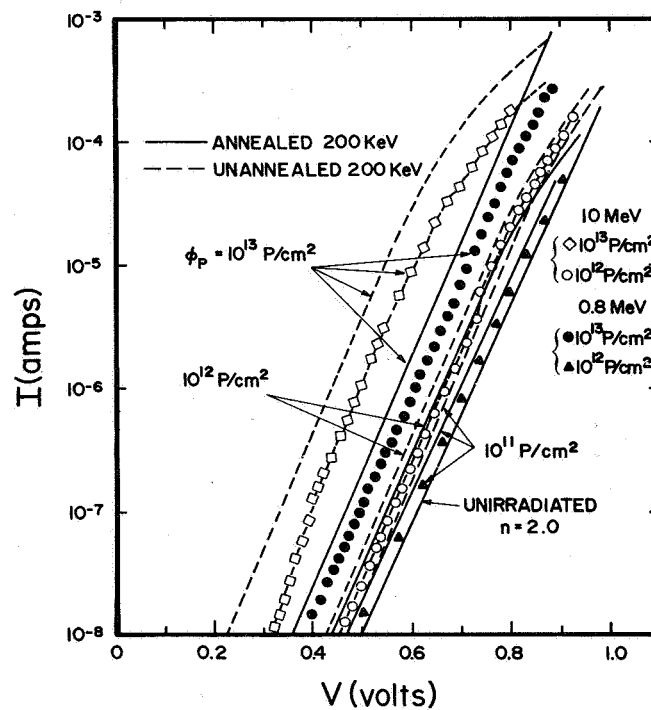


Fig. 6 Comparison of dark forward I-V characteristics for proton irradiated AlGaAs-GaAs solar cells, for different proton fluence and proton energy.

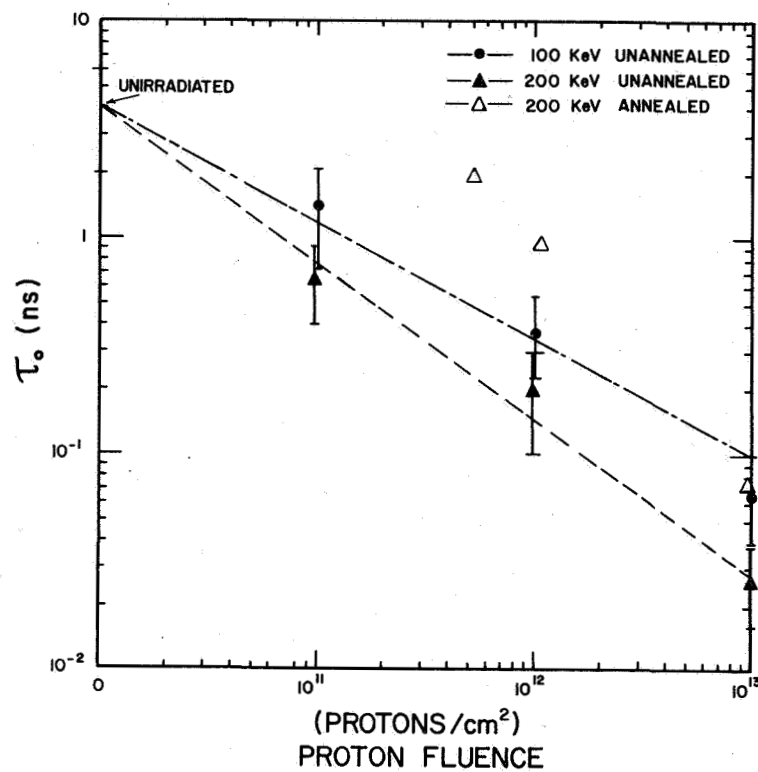


Fig. 7 Effective carrier lifetime vs proton fluence for the 100 and 200 KeV proton irradiated samples with and without thermal annealing. As calculated from the I-V data shown in Fig. 6.